

COMPARISON OF THE DIELECTRIC PROPERTIES FOR DOPED AND UNDOPED TiO₂ THIN FILMS

D. Mardare*, G. I. Rusu

"Al. I. Cuza" University, Faculty of Physics, 11 Carol I Blvd., R-6600, Iasi, Romania

The dielectric properties of TiO₂ thin films have been investigated on ITO/TiO₂/Au structures for a large domain of signal frequencies (10²Hz-10⁶Hz). At 100Hz, the values of the electric capacitance increases from 5.22nF to 22nF, by doping with Nb (0.35 at. %) and to 10.2nF by doping with Ce (0.4 at. %). This increase is correlated with the increase of the dielectric constant of the film. At 100 Hz, the dielectric constant increase from 83.6 for the undoped sample, to 179 by doping with Ce and to 108, by doping with Fe. Nb impurities determine a large increase of the dielectric constant, till 371, which is very important in fabricating capacitors. The dependence of dielectric loss versus frequency was also examined.

(Received September 25, 2003; accepted after revision February 9, 2004)

Keywords: Titanium dioxide, Polycrystalline thin films, Semiconducting films, Dielectric phenomena

1. Introduction

Due to their unusually high dielectric constant, titanium dioxide (TiO₂) thin films are attractive materials for a large number of important applications such as: high-density dynamic-memory devices, capacitors in microelectronics, insulator gate in MIS structures, etc. [1-3]. It is well known that impurity doping induces substantial modifications in electrical and optical properties of semiconductor materials, as shown in previous papers [4-6], for TiO₂ doped with Ce, Nb and Fe.

One of the most utilized methods for obtaining uniform and dense TiO₂ thin films, with well-controlled stoichiometry, is reactive sputtering [4-12].

The aim of this paper is to investigate how doping with some impurities like Ce, Nb and Fe can determine a change in their dielectric properties.

2. Experiment

Titanium dioxide films were deposited by r.f. (13.56 MHz) sputtering technique. Details on the deposition parameters are given elsewhere [4, 8]. The substrates used are glass covered by 100nm, transparent indium tin oxide (ITO) (from Merck Balzers).

The samples labeled by A, A_{Ce}, A_{Nb}, A_{Fe}, denote: pure TiO₂ sample, TiO₂ film doped with 0.40 at. % Ce, TiO₂ film doped with 0.35 at. % Nb and TiO₂ film doped with 1.00 at.% Fe, respectively.

X-ray diffraction (XRD) analysis was carried out with a Rigaku Geigerflex computer-controlled diffractometer (with Cu K_α radiation).

The surface morphology of the films was investigated by atomic force microscopy (AFM) in non-contact mode.

* Corresponding author: dianam@uaic.ro

Dielectric properties of ITO/TiO₂/Au structures were investigated using a Hewlett-Packard 4192A IMPEDANCE ANALYSER, on a frequency range of 10² Hz-10⁶ Hz, with a 0.1 V applied voltage.

In our experiments, the real and imaginary parts of the complex dielectric permittivity ϵ^* ($\epsilon^* = \epsilon - j\epsilon'$) were obtained with the assumption that studied cell is equivalent to a circuit consisting of an ideal capacitance C_p in parallel with a pure (ohmic) resistance R_p .

The capacitance of a parallel-plate capacitor is, for the real case, when the losses are present:

$$C = \epsilon_0(\epsilon - j\epsilon')S/d = \epsilon^* C_0 \quad (1)$$

where ϵ_0 is the absolute permittivity of the vacuum, ϵ is the dielectric permittivity of the thin film (the real part of the complex dielectric constant), ϵ' is the imaginary part of the complex permittivity, d is the distance between the plates, S is the area of a plate and C_0 is the capacitance of the empty cell ($C_0 = \epsilon_0 S/d$).

The dielectric permittivity is given by [13, 14]:

$$\epsilon = C_p/C_0 \quad (2)$$

The imaginary part of the complex permittivity can be expressed as:

$$\epsilon' = 1/(C_0 R_p 2\pi\nu) \quad (3)$$

The dielectric loss for this real capacitor is given by:

$$\tan\delta = G/(2\pi\nu C_p) = (2\pi\nu C_p R_p)^{-1} \quad (4)$$

where G is the electrical conductance and ν is the signal frequency.

By measuring C_p and R_p , eqs. (2), (3) and (4) permit to determine the values of ϵ , ϵ' and $\tan\delta$.

3. Results and discussion

From XRD measurements, discussed in detail in paper [4], a phase transition from rutile to anatase is observed by doping with Ce, Nb, and even with Fe, for these kind of TiO₂ films deposited onto ITO substrates (see Table 1).

Table 1. Impurities concentration, weight percentage of the anatase phase (W_A), thickness (d), surface roughness (R_{AFM}), dielectric permittivity (ϵ) at 10 kHz, electrical capacitance (C_p) at 100Hz, dielectric loss ($\tan\delta$) at 100 Hz.

Sample	Impurity Concentration	W_A (%)	d (nm)	R_{AFM} (nm)	ϵ	C_p (nF)	$\tan\delta$
A	-	54	300	5.5	60	5.2	2.20
A _{Ce}	0.40 at. % Ce	80	300	5.4	77	10.2	0.27
A _{Nb}	0.35 at. % Nb	83	300	5.0	311	22.0	37.00
A _{Fe}	1.00 at. % Fe	65	250	9.2	72	6.4	0.68

AFM measurements, as well as variable-angle spectroscopic ellipsometry (VASE) measurements [5,6], evidence relatively smooth surfaces (Table 1). Doping with Fe increases the surface roughness, R_{AFM} , while doping with Nb and Ce doesn't practically modify it. This conclusions are also confirmed by SEM images [4].

We have investigated the dependences of the dielectric permittivity (dielectric constant), dielectric loss and electrical conductance versus frequency (Figs. 1-3).

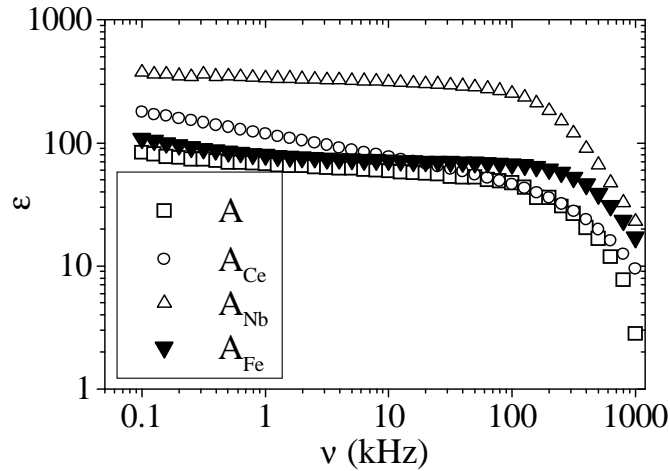


Fig. 1. Dielectric permittivity (ϵ) versus signal frequency.

From Fig. 1 it can be observed that, in domain of lower frequency, the dielectric constant slowly decreases with increasing frequency till a value of frequency, different for each sample. Then follows a sharp decrease explained by an incomplete polarization (the electrical dipoles can not follow the variation of the electric field anymore). For sample A, this sharp decrease begins at 100 kHz, for A_{Nb} it begins at 125 kHz, and for A_{Fe} at 250 kHz. At a signal frequency of 100 Hz, the dielectric constant increases from 83.6 for the undoped sample, to 179 by doping with Ce and to 108, by doping with Fe. The mentioned values of the dielectric constants, obtained for the samples A and A_{Fe} , are in agreement with those obtained by Bally et al. [8]. Nb impurities determine a large increase of the dielectric constant, till 371. The structural differences explain these variations in the dielectric constant.

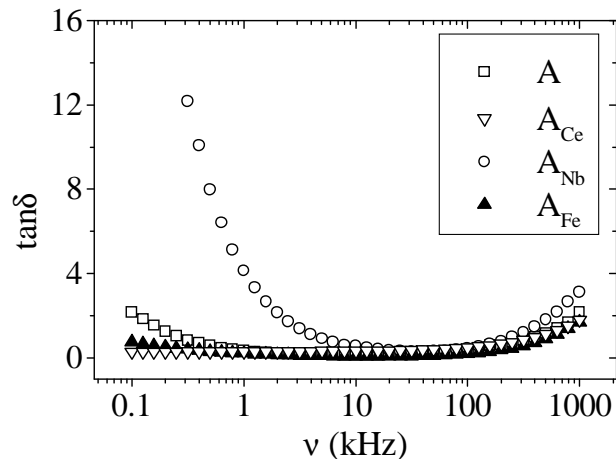


Fig. 2. Dielectric loss ($\tan\delta$) versus signal frequency.

In low signal frequency range, when the electrical dipoles are able to follow the variation of the electric field, the dielectric loss decreases with the increases of signal frequency (Fig. 2), since the electrical capacitance and conductance are almost constant on this range (Figs. 1 and 3). Exception is made for the Ce doped sample where a slight increase in dielectric loss appear. A common palier is observed of the studied samples, ranging between 10 kHz and 100 kHz, where $\tan\delta$ does not depend

on frequency, having the lowest values: 0.1-0.3. In this signal frequency range, whose limits are different from one sample to another, the electrical conductance increases with the frequency, a common observation for many dielectrics [15]. For these low values of $\tan\delta$, it may be considered that we can obtain the most precise values for the dielectric constant. At 10 kHz, the values of ϵ are: 60, 77, 311, 72, for samples A, A_{Ce} , A_{Nb} , A_{Fe} , respectively.

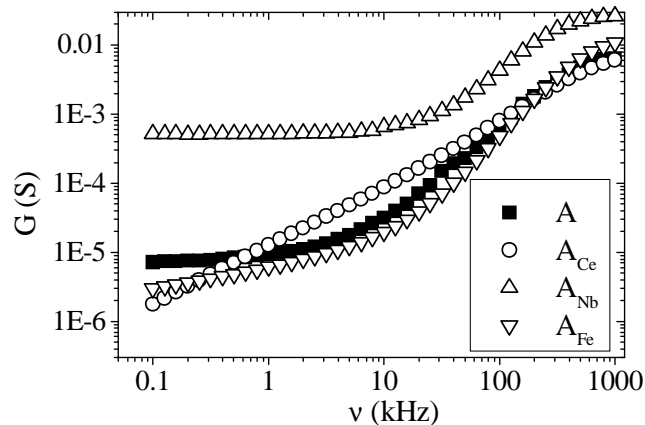


Fig. 3. Electrical conductance (G) versus signal frequency.

4. Conclusions

In this paper we have shown that dielectric properties are modified by doping, as a consequence of changing of films structure. Nb doping induce a large increase of the dielectric constant which is very important for fabricating capacitors in microelectronic devices.

Acknowledgements

We would like to thank Prof. F. Lévy and A. Bally from Institute of Applied Physics, EPFL Lausanne, Suisse for providing the necessary laboratory facilities to carry out this investigation.

References

- [1] P. J. Martin, *J. Mater. Sci.* **21**, 1 (1986).
- [2] W. D. Brown, W. W. Grannemann, *Solid State Electron* **21**, 837 (1978).
- [3] T. Fuyuki, H. Matsunmi, *Jpn. J. Appl. Phys.* **25**, 1288 (1986).
- [4] D. Mardare, M. Tascu, M. Delibas, G. I. Rusu, *Appl. Surf. Sci.* **156**, 200 (2000).
- [5] D. Mardare, P. Hones, *Mater. Sci. Eng.* **B68**, 42 (1999).
- [6] D. Mardare, G. I. Rusu, *Mater. Sci. Eng.* **B75**, 68 (2000).
- [7] D. Mardare, G. I. Rusu, *Phys. Low-Dim. Struct.* **11/12**, 69 (1999).
- [8] A. R. Bally, E. N. Korobeinikova, P. E. Schmid, F. Lévy, F. Bussy, *J. Phys. D: Appl. Phys.* **31**(10), 1149 (1998).
- [9] D. Mardare, A. Stancu, *Mater. Res. Bull.* **35**, 2017 (2000).
- [10] D. Mardare, G. I. Rusu, *Materials Letters* **56/3**, 210 (2002).
- [11] L. J. Meng, M. P. Dos Santos, *Thin Solid Films* **226**, 22 (1993).
- [12] D. Mardare, C. Baban, R. Gavrilă, M. Modreanu, G. I. Rusu, *Surf. Sci.* **507-510**, 468 (2002).
- [13] T. Furukawa, M. Imura, H. Yuruzume, *Jpn. J. Appl. Phys.* **36**, 1119 (1997).
- [14] Y. Cui, J. Wu, N. Kamanina, A. Pasaje, A. Leyderman, A. Barrientos, M. Vlase, B. G. Penn, *J. Phys. D: Appl. Phys.* **32**, 3215 (1999).
- [15] L. Maissel, R. Glang (Eds.), *Handbook of Thin Film Technology*, (McGraw-Hill, New York, 1970).